AIAA JOURNAL
Vol. 45, No. 7, July 2007

Load Updating for Nonlinear Finite Element Models

Jing Li* and Rakesh K. Kapania†
Virginia Polytechnic Institute and State University, Blacksburg, Virginia 24061-0203

DOI: 10.2514/1.19073

A measurement-based load updating method for finite element models subjected to static loads was studied using a four-noded curved beam element for large displacements/rotations and a gradient-based variable metric optimizer. Finite element analysis was used to numerically calculate the geometrically linear and nonlinear responses and their sensitivities under a given load. The optimizer was used to recursively update the load so that it minimized the square of the difference between the calculated and prefiltered/noise-free measured (displacement or strain) data. For the basic studies, the extracted load was represented within an element by a linear combination of integrated Legendre polynomials, the coefficients of which were taken as design variables of the least-squares problem. Through a model order analysis, the benefits for solving load updating problems using the relative deformation measurement, the polynomials of lower orders, the elements of larger sizes (because of using the high precision four-noded beam element), and the denser measured points were studied for linear responses under different types of applied loads. It was confirmed that using the reduced number of unknown variables to obtain an *overdetermined inverse problem* helps get unique and stable extracted loads. Though this conclusion was verified mainly through illustrative examples for a cantilever beam, it was generally applicable to other load updating or inverse problems. Further examples were given for a three-dimensional portal frame load updating, extracting highly oscillating loads, and a strain-based cantilever beam load updating. The final examples were load updating for geometrically nonlinear finite element models under self-weight, snow, and/or pressure loads.

I. Introduction

FINITE element analysis (FEA) has long been one of the generally accepted tools for structural analysis. Although differences between real testing and FEA are usually reduced using system identification, much effort has been focused on the increasing accuracy of the mathematical model of the structure from the point of view of updating the finite element model (FEM) of the structure itself under given applied loads.

However, simply updating the FEM itself is not sufficient to satisfactorily reduce the differences between the observed experimental data and numerically calculated results based on FEA if the applied loads are not exactly known. Also, operational loads, such as self-weight, snow, waves, winds, etc., either dynamic or static, are usually not simply or directly measurable. Therefore, it is an appealing alternative to use the indirect or inverse method to determine or update the approximate applied loads based on actually measured responses of the structure under realistic working conditions by identifying load parameters of the established load model. In other words, we seek to reduce those differences by modifying not the FEM of the structural system, but the loading that the structure is subjected to such that the experimental and the finite element responses match in the least-squares sense (Rattray et al. [1], Avitabile [2], Chock and Kapania [3]).

The load updating is a special application of system identifications in the growing field of inverse problems, which arise whenever one searches for causes of observed or desired effects (Engl and Kugler [4]). Therefore, an examination of the literature in terms of inverse problems aids us in determining the most appropriate methodology for load updating.

In most formulations, the load identification process requires the inversion of the global matrix, which tends to be very ill conditioned. That is, very small errors in measurements propagate into large errors in estimated forces, especially at frequencies close to the resonance and antiresonance conditions (Starkey and Merrill [5]). On the other hand, in many practical inverse problems, one aims to retrieve a model that has infinitely many degrees of freedom from a finite amount of data, which leads to the nonuniqueness of the solutions of the *rank-deficient* or *underdetermined* problems (Schulze [6], Eriksson and Gulliksson [7]). Therefore, solving an inverse problem entails more than estimating a model: any inversion is not complete without a description of the class of models that is consistent with the data (Snieder [8]).

The progress to overcome this difficulty is called regularization, which is used to replace an ill-posed problem by a family of neighboring well-posed problems (Engl and Kugler [4]) or filter out the influence of noise (Hansen and O'Leary [9]).

The singular-value decomposition (SVD) technique (Elliott et al. [10], Chock and Kapania [3]) along with the pseudoinverse technique (Fabunmi [11]) provides the fundamental theory and methods to overcome ill-conditioning for most linear inverse problems. The pure SVD method gives a direct solution of a direct least-squares formulation. Associated with the SVD technique are two well-known regularization methods for linear inverse problems, the Tikhonov regularization (due to Tikhonov and Arsenin [12]) and the truncated singular-value decomposition (Hansen and O'Leary [9], Engl and Kugler [4]). The Tikhonov regularization is to add a constraint term to the pure least-squares formulation, an approach that can be readily extended to the solution of the nonlinear inverse problems. The truncated SVD method is to truncate off all the terms of zero or close-to-zero singular values.

Smoothing or filtering either the (noisy) data or the (oscillating) solution (Louis [13]), using overspecified or overdetermined boundary data for complete data (Andrieuxy and Ben Abda [14]) and many boundary measurements (Eller [15]), are alternative and intuitive approaches to regularize the ill-posed inverse problems, and overcome oscillating, arbitrary, and/or unique solution problems. A priori information (Sabatier [16], Kaipio et al. [17]) and richly measured or experimental data helps one to establish unique results or solve identification problems.

Presented as Paper 1646 at the 45th AIAA/ASME/ASCE/AHS/ASC Structures, Structural Dynamics & Materials Conference, Palm Springs California, 19–22 April 2004; received 24 July 2005; revision received 28 November 2006; accepted for publication 5 January 2007.

*Graduate Research Assistant, Department of Aerospace and Ocean Engineering; Currently Research Associate, Department of Mechanical Engineering, Oakland University, Rochester, MI 48309; li2@oakland.edu. Member AIAA.

†Professor, Department of Aerospace and Ocean Engineering; rkapania@vt.edu. Associate Fellow AIAA.

A regularization effect can already be obtained by a finite-dimensional approximation of the problem, where the approximation level plays the role of the regularization parameter (Engl and Kugler [4]). At least for severely ill-posed problems the dimension of the problem has to be low to keep the total extracted error small (Engl and Kugler [4]). The number of zero singular values increases when the size of the inverse problem increases (Hansen and O'Leary [9]). For this reason, the formulation of the inverse problems, for example, load updating or identification on the discrete setting, such as based on FEM, is advantageous. The FEM often includes a large number of degrees-of-freedom (DOF), although most of them are not necessarily needed, especially those to which no forces are applied and those for which no responses are measured. To estimate the loads, the FEM has to be reduced by model reduction techniques so that responses need only be measured at a limited number of sites (Chen and Geradin [18]).

For almost all inverse problems, optimization is not only a formulation, but also a solution technique. Ewing et al. [19], Rattray et al. [1], Ring [20], Avitabile [2], and Chock and Kapania [3] were concerned with or used least-squares formulation, which is to define an error that characterizes the quality of the model with respect to the experimental data and then to minimize this error. In solving their inverse problems, Dunn , Chiroiu et al. [22], and Trivailo et al. [23,24] used the neural networks and genetic algorithms; Hanke [25], Rieder [26], Burger and Muhlhuber [27], Chock and Kapania [3], and Feijoo et al. [28] used gradient-based methods.

Although a nonlinear inverse problem is usually solved by the iterative algorithms (Engl and Kugler [4]), including various optimization methods, its ill-posedness may be more severe than for linear problems as nonlinear error propagation is a difficult problem (Snieder [8]). In the field of elasticity or structures, examples of handling nonlinear inverse problems were given by Ewing et al. [19] for nonlinear beam cross-sectional property estimation, Chiroiu et al. [22] for material constants extraction, Hasanov and Mamedov [29] for identifying elastoplastic properties of a plate, and Ring [20] for load identification.

The identification of applied loads using measured response is not a new concept. We can easily list some early works in the literature. Pilkey and Kalinowski [30] dealt with identification of shock and vibration forces. Hillary and Ewins [31] were concerned with the use of strain gauges in force determination and frequency response function measurements. Gregory et al. [32] studied experimental determination of the dynamic forces acting on nonrigid bodies. Stevens [33] presented an overview on force identification problems. Wang et al. [34] coped with force identification from structural response. Starkey and Merrill [5] addressed the ill-conditioned nature of indirect force-measurement techniques.

Besides, the following earlier and recent works may present a clear picture in the field of load updating or identification for structures.

Park and Park [35] dealt with transient response of an impacted beam and indirect impact force (location and time history) identification using wave propagation theory and strain measurements.

Chen and Geradin [18] identified the dynamic force for beamlike structures by dividing the entire structure into substructures according to the excitation locations and the measured response sites, and then represented each substructure by an equivalent element. Therefore, the resulting model only retained the DOF associated with the excitation and the measured responses and the DOF corresponding to the boundaries of the structures. They tried to avoid the processes of modal parameter extraction, global matrix inversion, and model reduction.

Johnson [36] used system informatics to derive necessary and sufficient conditions to ensure convergence of the loads determined by solving the underlying inverse problem. On the basis that a system is a superposition of signals, (Johnson [37]) developed a force and moment identification method using basis functions chosen to represent desired characteristics of time variations of loadings in a general class of linear (linearized) dynamic and vibration problems with multiple-inputs and multiple-measurements. Johnson [38] applied the preceding developed methodologies to the identification of the unknown, immeasurable static load distributions on beams, from measurements of beam static deflections. He noted the difficulties in identifying a system near the applied boundary conditions and presented a method for inverse problem solutions.

Ring [20] identified the unknown load for a steel-concrete composite beam using the measured inclination (or slope) along the axis of the beam. A nonlinear, nonsmooth constitutive relation was used to model the partial breaking of the pile at points where the bending moment exceeds a critical value. A two-step approach for the inverse problem was considered. In the first step, the broken and unbroken parts of the beam were determined from the solution of a regularized least-squares problem, where a total variation type regularization term was used. In the second step, a linearly constrained least-squares problem was solved. Existence, stability, and convergence results were presented.

Law and Fang [39] used the dynamic programming technique to overcome a common weakness of large fluctuations in the identified load results. The forces in the state-space formulation of the dynamic system are identified in the time domain using a recursive formula based on several distributed sensor measurements, and responses of the structure are reconstructed using the identified forces for comparison. Like all inverse problems, the computation is ill conditioned. However, the dynamic programming technique inherently provides bounds to the ill-conditioned forces.

Chock and Kapania [3] addressed the importance of load updating for FEM and its application in engineering. They gave a relatively extensive survey of the load updating relevant literature in the time domain as the literature for static load updating was rare. They applied the achievements in time domain to the static load updating problem, and especially dealt with the load updating for linear FEM of one-dimensional beam problems. The classical least-squares fitting method was used to minimize the error between the measured and analytical displacements. The load distribution was taken elementwise and assumed to be the linear combination of integrated Legendre polynomials with the coefficients as the known parameters to be identified. The conditioning number of the resulting system equations was examined and provided a solution method more robust through the use of singular-value decomposition. This work was extended from a one-dimensional beam to a two-dimensional plate and initial results on the plate were discussed (Chock and Kapania [40]).

Padmanabhan et al. [41] presented a method for load and boundary condition calibration using full-field strain measurement by minimizing the least-square error between the strains computed using the finite element model and the strains and displacements obtained experimentally. The nodal loads and the compliance at fixed boundaries are treated as the variables in the optimization problem. The compliance is modeled as springs attached at the nodes that are on the boundary where the structure is restrained. The method is verified by computing the loads and boundary conditions when displacements, maximum shear strain, or both are available at a large number of points on the surface of the structure. The experimental data set was generated using the luminescent photoelastic coating technique.

Our current work presents load identification/updating for geometrically nonlinear FEM of beams and frames subjected to static loading, modeled by using a four-noded curved beam element (Kapania and Li [42,43]). Using this element makes it possible to have a system of lower dimension as it requires fewer elements to predict the responses in higher precision and makes solving the hard nonlinear inverse problems easier for the given but limited data points if the number of the unknown load parameters is proportional to the number of elements.

The optimizer L-BFGS-B (Byrd et al. [44], Zhu et al. [45]), a limited-memory quasi-Newton code for large-scale *bound-constrained* or unconstrained optimization, is used to solve the *preconditioned* least-squares problem. Though the bound-constraints on the design variables could play an important role in the regularization, this capability is not addressed for the current studies. A unique solution for an underdetermined system, however, is obtained numerically using this iteration-based optimizer by

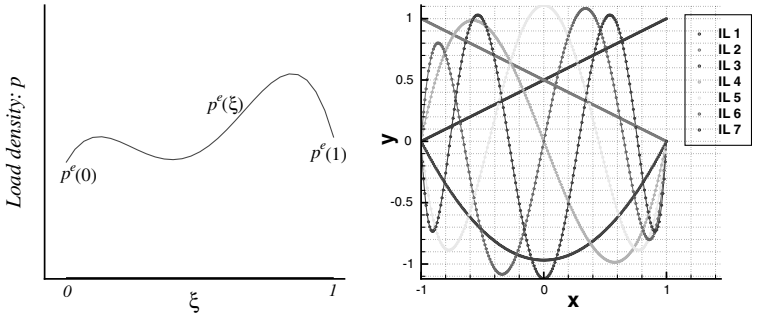

a) Load density distribution along a beam element axis

b) First seven integrated Legendre polynomials

Fig. 1 Load distribution within an element as a linear combination of integrated Legendre polynomials.

starting from an approximate uniform load determined by a priori information. If the information is not known a priori, the approximate load is assumed to vanish. Starting from a uniform load with a small design stepsize can prevent the procedure from stopping at a wildly oscillating solution.

Simplified static load models for self-weight, snow, and pressure loads (Kapania and Li [43]) with uniform, linear, or sinusoidal distribution are used for assumed operational loads at the global level. For the basic studies on the load updating, the extracted applied load is represented *elementwise* by a linear combination of the integrated Legendre polynomials, though an *across-element* representation of the load is recommended for further studies to avoid the oscillations in the solution by reducing the unnecessary inverse problem model DOF. The coefficients of integrated Legendre polynomials are the parameters to be extracted using measured displacements or strains.

We assume that the measured data are noise-free, and therefore do not directly use the general Tikhonov-like regularization, though we could use it for the underdetermined system to have a unique solution. For the basic studies, however, we address the benefits for solving the load updating problems using the relative measurement method, the fewer four-noded cubic beam elements, polynomials of lower order for load representation within an element, and richer sparsely measured data, smoothing, and enforcing C^0 continuity to reduce the model order to the extent that an overdetermined inverse problem is obtained.

Illustrative examples of linear and nonlinear FEM are given for beams in planar loading cases and a portal frame for a three-dimensional loading case. All noise-free measured data are artificially created from calculation based on FEM under a reference applied load.

II. Theory

A. Load Representation Within an Element

Because we are concerned with externally applied load identification or load updating for finite element models, it is necessary to parameterize the unknown applied loads. Using nodal loads may be a direct choice for the unknown loading, but when the number of nodes for the FEM is large, the number of unknown nodal loads will be large as well. This will increase the effort to extract the applied loads. Because the measured data are often limited along certain DOF at some of the FEM nodes, and the number of the measured data may be less than the number of extracted nodal loads, the problem will be explicitly underdetermined. Therefore, considering the fact that in real engineering problems, the external load distributions are not subject to the finite element mesh and software used, we may better choose to parameterize the load distribution in a way different from that in the finite element model. Although we can represent the load distribution across-elementwise, in this study, however, we limit the applied load distribution elementwise to simplify and generalize the formulation. A concentrated load is considered as a special case of the distributed load.

Assume that a load density function $p(\xi)$ ($\xi \in [0, 1]$) over the beam element (Fig. 1a) can be represented by a linear combination of a set of basis functions $P_\alpha(\xi)$:

$$p(\xi) = \sum_{\alpha=1}^{N_c} c_\alpha P_\alpha(\xi) \tag{1}$$

Here, c_α are unknown load coefficients. It should be understood that though increasing the number N_c of basis functions over an element will allow a more accurate representation of the element loading, it has its limits due to the accuracy and resolution of the element used. Therefore, there is a need to study how many terms should be used to obtain a balance between the precision of the load representation and the capability to achieve the desired precision.

In this study, we follow the work by Chock and Kapania [3], and use integrated Legendre polynomials as basis functions to represent the load distribution within an element. Refer to Fig. 1b and Appendix A for the shapes and definitions of the first seven integrated Legendre (IL) polynomials, respectively. (IL 0 can be an extension to represent a constant distribution, though it can represent the combination of IL 1 and IL 2.) It can be seen from Fig. 1b that the coefficients of the first two terms of $P_\alpha(\xi)$ ($\alpha = 1, 2$) in Eq. (1) are the load density values at the two ends of the element. However, all higher terms of $P_\alpha(\xi)$ ($\alpha > 2$) vanish at the two ends and, therefore, they are used as *bubble functions (interior modes)* (Solin [46]) for p-element (Szabo and Babuska [47]) or p-adaptability. We intend to use for the basic studies, with respect to the order of polynomials, from constant, linear, quadratic, cubic, and any higher order regardless of the number of nodes within an element. The first two terms are used to represent any linearly distributed load, and all intended higher terms can be used for nonlinear load distribution regardless the number of nodes in an element. To be specific in this paper, the number of nodes in an element is four. The load distribution within an element is, however, independent of its interior nodes, not limited to a cubic nodal Lagrangian shape as it is used for the four-noded beam element formulation. Though it is not the only choice, using integrated Legendre polynomials is a convenience for the basic studies with respect to the order of the polynomials and demonstrate that a lower order of polynomials than the cubic shall be used.

B. Load Updating for Nonlinear FEM

In general, for our geometrically nonlinear FEM in the three-dimensional case, we can start with the state equation of a nonlinear structural system (Kapania and Li [43]):

$$\boldsymbol{R}(\boldsymbol{a}, \boldsymbol{c}, \lambda) = \boldsymbol{q}_{\text{int}}(\boldsymbol{a}) - \lambda \boldsymbol{q}_{\text{ext0}}(\boldsymbol{a}, \boldsymbol{c}) = 0 \tag{2}$$

where $\boldsymbol{R}$ is the residual vector, $\boldsymbol{q}_{\text{int}}$ the nodal internal force vector, $\boldsymbol{q}_{\text{ext0}}$ the nodal external load vector calculated at the applied load level, λ the proportional nodal loading factor, $\boldsymbol{a} = \boldsymbol{a}(\boldsymbol{c}, \lambda)$ the nodal displacement vector, and $\boldsymbol{c}$ the load (force) coefficient vector, which is further determined by the unknown load design (coefficient) vector $\boldsymbol{x}$ with independent components. Now, we have the global entities in

component forms:

$$\boldsymbol{R} = \begin{bmatrix} R_1 \\ R_2 \\ \vdots \\ R_{N_a} \end{bmatrix}, \qquad \boldsymbol{q}_{\text{int}} = \begin{bmatrix} q_{\text{int1}} \\ q_{\text{int2}} \\ \vdots \\ q_{\text{int}N_a} \end{bmatrix}, \qquad \boldsymbol{q}_{\text{ext0}} = \begin{bmatrix} q_{\text{ext01}} \\ q_{\text{ext02}} \\ \vdots \\ q_{\text{ext0}N_a} \end{bmatrix}$$
$$\delta\boldsymbol{a} = \begin{bmatrix} \delta a_1 \\ \delta a_2 \\ \vdots \\ \delta a_{N_a} \end{bmatrix}, \quad \text{and} \quad \boldsymbol{x} = \begin{bmatrix} x_1 \\ x_2 \\ \vdots \\ x_{N_x} \end{bmatrix} \tag{3}$$

Note that $N_a \equiv N_{\text{dof}}$, the total DOF of the finite element system; N_x is the total number of the independent load (force) coefficients or unknown load design variables.

Let $\boldsymbol{a}_m$ represent the measured displacement response and $\boldsymbol{a}$ the calculated displacement response. The square of the error E_a is given as

$$E_a = \frac{1}{2m}\boldsymbol{e}^t\boldsymbol{e} \tag{4}$$

where the vector $\boldsymbol{e}$ is defined as

$$\boldsymbol{e} = \boldsymbol{a} - \boldsymbol{a}_m \tag{5}$$

and m is the number of the measured data. Because the response can be measured only at a limited number of points, the dimensions of vectors $\boldsymbol{a}$ and $\boldsymbol{a}_m$ will be different. We have to reduce the dimension of $\boldsymbol{a}$ to that of $\boldsymbol{a}_m$ if we consider $\boldsymbol{a}_m$ to be fully populated. Thus, we can use a transformation matrix T onto $\boldsymbol{a}$, so that Eq. (4) becomes

$$E_a = \frac{1}{2m}||T\boldsymbol{a} - \boldsymbol{a}_m||_2^2 = \frac{1}{2m}\boldsymbol{e}^t\boldsymbol{e} \tag{6}$$

where the vector $\boldsymbol{e}$ is defined as

$$\boldsymbol{e} = T\boldsymbol{a} - \boldsymbol{a}_m = \begin{bmatrix} a_{I_1} - a_{mI_1} \\ a_{I_2} - a_{mI_2} \\ \vdots \\ a_{I_m} - a_{mI_m} \end{bmatrix} \tag{7}$$

where subscript indices $I_1, I_2, \ldots, I_m$ give the corresponding locations at the array $\boldsymbol{a}$. An alternative way to measure the error is in the relative sense,

$$\bar{\boldsymbol{e}} = \begin{bmatrix} \frac{a_{I_1}}{a_{mI_1}} - 1 \\ \frac{a_{I_2}}{a_{mI_2}} - 1 \\ \vdots \\ \frac{a_{I_m}}{a_{mI_m}} - 1 \end{bmatrix} \tag{8}$$

which makes smaller measured displacements and their gradients treated equally, or they would be ignored because of being truncated off due to the limited machine precision. We can relate $\bar{\boldsymbol{e}}$ to $\boldsymbol{e}$ by

$$\boldsymbol{e} = D_{a_m}\bar{\boldsymbol{e}} \quad \text{or} \quad \bar{\boldsymbol{e}} = D_{a_m}^{-1}\boldsymbol{e} \tag{9}$$

where

$$D_{a_m} = \begin{bmatrix} a_{mI_1} & 0 & \cdots & 0 \\ 0 & a_{mI_2} & \cdots & 0 \\ \vdots & \vdots & \ddots & \vdots \\ 0 & 0 & \cdots & a_{mI_m} \end{bmatrix} \quad \text{or}$$
$$D_{a_m}^{-1} = \begin{bmatrix} \frac{1}{a_{mI_1}} & 0 & \cdots & 0 \\ 0 & \frac{1}{a_{mI_2}} & \cdots & 0 \\ \vdots & \vdots & \ddots & \vdots \\ 0 & 0 & \cdots & \frac{1}{a_{mI_m}} \end{bmatrix} \tag{10}$$

Now, the least-squares problem of the load updating for the nonlinear FEM is to find the load (force) coefficient vector $\boldsymbol{x}$ that will minimize

$$E = E_a \tag{11}$$

which requires that the variation of E with respect to $\boldsymbol{x}$ vanish, noticing Eq. (C10) in Appendix C

$$\delta_x E = \frac{1}{m}\boldsymbol{e}^t\delta_x\boldsymbol{e} = \frac{1}{m}\boldsymbol{e}^t T\delta_x\boldsymbol{a} = \frac{1}{m}E_{,\boldsymbol{x}}\delta\boldsymbol{x} = 0 \tag{12}$$

or equivalently, the sensitivity of the square of the displacement response error with respect to load (force) coefficient vector $\boldsymbol{c}$ or $\boldsymbol{x}$ to vanish

$$E_{,\boldsymbol{x}} = \boldsymbol{e}^t\boldsymbol{e}_{,\boldsymbol{x}} = 0 \tag{13}$$

$$\boldsymbol{e}_{,\boldsymbol{x}} = T\boldsymbol{a}_{,\boldsymbol{x}} \tag{14}$$

where $\boldsymbol{a}_{,\boldsymbol{x}} = \lambda K_T^{-1}\boldsymbol{q}_{\text{ext0},\boldsymbol{x}}$, as given in Eq. (C11) of Appendix C, is the sensitivity of the displacement vector $\boldsymbol{a}$ with respect to the load (force) coefficient vector $\boldsymbol{x}$, K_T is the tangent stiffness matrix, and $\boldsymbol{q}_{\text{ext0},\boldsymbol{x}}$ is the global load (force) coefficient matrix, assembled from element force coefficient matrices as given in Eqs. (B15–B21) of Appendix B.

For linear FEM, K_T^{-1} is constant and therefore $\boldsymbol{e}_{,\boldsymbol{x}}$ is constant with respect to the load (force) coefficients. Equation can be transformed to a linear equation system with symmetric coefficient matrix. For the geometrically nonlinear FEM, however, the relationships between responses and loads are no longer proportional, i.e., K_T^{-1} and $\boldsymbol{e}_{,\boldsymbol{x}}$ are no longer constant. Therefore, one needs to recursively solve a nonlinear system state equation within an unconstrained nonlinear programming problem or sequential unconstrained nonlinear programming problems as described in Eq. (11). In each load updating step, one must reanalyze the geometrically nonlinear problem for both structural responses and their sensitivities with respect to the load (force) coefficients.

The ARCHCODE, a FORTRAN FEA code with the four-noded curved beam element first implemented in Kapania and Li [43], is extended and used to predict the linear and geometrically nonlinear responses and their sensitivities with respect to the load coefficients.

C. Constraints on Load Distribution

The load updating problem usually has an infinite number of solutions due to the rank-deficient and underdetermined nature of the inverse problem. Most of the solutions may not be practical or useful for the realistic applications at hand. Therefore, it is often necessary to set certain constraints on the load distribution. For example, if we know beforehand that the load over an element should be smooth or close to a linear distribution, and/or the load across two adjacent beam elements should be continuous or almost continuous, we can enforce load smoothing within an element and/or C^0 continuity across two adjacent elements. Then, the objective function of the scaled (Banks [48]) and mixed (Ewing et al. [19]) least-squares problem in Eq. (11) becomes

$$E = \lambda_a E_a + \lambda_T E_T + \lambda_S E_S + \lambda_{C^0} E_{C^0} \tag{15}$$

where

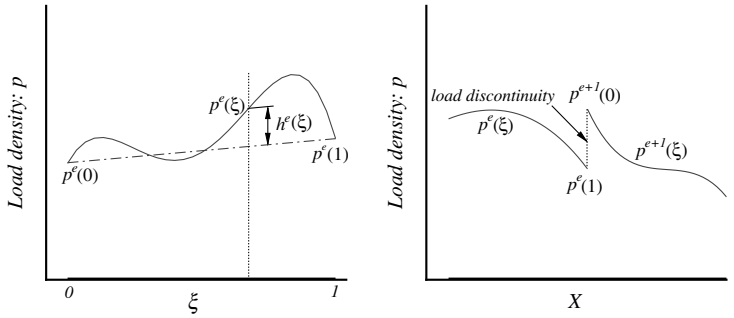

a) Linear load density distribution along a beam element axis **b) Load discontinuity between two adjacent elements**

Fig. 2 Need for constraints on the extracted load.

$$E_T = \frac{1}{2N_{\text{elm}}} \sum_{e=1}^{N_{\text{elm}}} \int_0^1 [p^e(\xi) - p^{e*}(\xi)]^2 \mathrm{d}\xi \tag{16}$$

is the general term for the Tikhonov regularization to handle both the noisy data problem and the nonunique solutions problem, and reflects the average value of the difference between the predicted load distribution $p^e(\xi)$ and the approximate one $p^{e*}(\xi)$[‡] (Banks [48], Eriksson and Gulliksson [7]):

$$E_S = \frac{1}{2N_{\text{elm}}} \sum_{e=1}^{N_{\text{elm}}} \int_0^1 [p^e(\xi) - (1-\xi)p^e(0) - \xi p^e(1)]^2 \mathrm{d}\xi \tag{17}$$

is the smoothing term, and reflects the average value of the extracted load error $h^e(\xi)$ compared with the linear distribution over an element, as seen in Fig. 2a, and

$$E_{C^0} = \frac{1}{2(N_{\text{elm}} - 1)} \sum_{e=1}^{N_{\text{elm}}-1} [p^e(1) - p^{e+1}(0)]^2 \tag{18}$$

reflects the average load discontinuity between two adjacent elements, as seen in Fig. 2b. (X is the global coordinate of the beam axis.) The least-squares scale factor is λ_a, and λ_T, λ_S, and λ_{C^0} are the corresponding multipliers or regularization factors for the Tikhonov regularization term E_T, smoothing term E_S, and C^0 continuity term E_{C^0}, respectively. Note that E_S and E_{C^0} are special cases of the general Tikhonov regularization term E_T. Though both the effect of the noise in the measured data can be filtered out and a smooth unique solution can be obtained using the general Tikhonov regularization, in this study, however, the noise in the measured data is not considered as we address the benefits for solving the load updating problems using the relative measurement, fewer four-noded beam elements, polynomials of lower order, and richer measured data, solution smoothing (Louis [13]), and enforcing C^0 continuity.

The optimizer L-BFGS-B (version 2.1) (Zhu et al. [45], Byrd et al. [44]), a limited-memory quasi-Newton code for large-scale bound-constrained or unconstrained optimization, is used to solve the scaled and mixed least-squares (LSQ) problem Eq. (15). Though the bound-constraints on the design variables could play an important role in the regularization, this capability is not addressed for the current studies. A unique solution for the underdetermined system (when a Tikhonov regularization is not used) is obtained numerically using this iteration-based optimizer by starting from an approximate *uniform load* determined by a priori information. If the information is not known a priori, the approximate load is assumed to *vanish*. Starting from a uniform load with a small design stepsize can prevent the procedure from stopping at a wildly oscillating solution.

[‡]For a classical Tikhonov regularization method, the approximate applied load term is assumed to be $p^{e*}(\xi) = 0$. If an approximate applied load is known from a priori information, the extracted load may be closer to the actual applied load for a given regularization effect.

III. Examples

In all the numerical examples for the solutions of the LSQ problem Eq. (15) by the optimizer L-BFGS-B, the initial design variables are uniformly set to *zero*, which means the load updating procedure starts at a zero level load.

Unless mentioned otherwise, no Tikhonov regularization is used, i.e., $\lambda_T = 0$, $\lambda_S = 0$, and $\lambda_{C^0} = 0$.

The procedure terminates if 1) the total number of the function E and the gradient $E_{,\boldsymbol{x}}$ evaluations exceeds 999, or 2) the *projected gradient* proj$E_{,\boldsymbol{x}}$ (Zhu et al. [45], Byrd et al. [44]) is small enough: $|\text{proj}E_{,\boldsymbol{x}}|/-(\lambda_a + |E|) < \varepsilon_g$, or 3) the function value E is small enough: $|E|/\lambda_a \le \varepsilon_f$. Then, the procedure is considered converged. The parameters are chosen as follows except when stated otherwise: $\lambda_a = 1 \times 10^{14}$, $\varepsilon_g = 1 \times 10^{-14}$, $\varepsilon_f = 1 \times 10^{-3}$, and the machine precision of the computer (Intel Pentium 3, 600 MHz, 128 MB RAM) is $\varepsilon_M = 2.22 \times 10^{-16}$. Referring to Eq. (15), we know that E is the scaled least squares, λ_a is the scalar of the squared difference between the calculated and measured deformations, and ε_g and ε_f are, respectively, the relative tolerances of proj$E_{,\boldsymbol{x}}$ with respect to $\lambda_a + |E|$ and E with respect to the scalar λ_a.

In addition to the preceding termination criteria, for nonlinear examples, the procedure stops when the step size $||\boldsymbol{x}_{\text{current}} - \boldsymbol{x}_{\text{previous}}||_2 \le \varepsilon_{\text{step}} = 1 \times 10^{-3}$.

For this fundamental study, we do *not* use actually measured data. Instead, we will use the *calculated* deformation (later/axial displacements or strains) from FEA under a reference applied load as the noise-free measured data. The extracted load direction is known a priori. In the load updating procedure, the load distribution within an element is represented by the linear combination of up to six integrated Legendre polynomials Although within the four-noded curved beam FEA procedure, the load distribution is always represented by cubic Lagrangian interpolation of the four nodal values.

In the results of all the examples, described in the following, X, Y, and Z are the position coordinates of the beam or frame in a three-dimensional space. Displacements share the same scale as the position coordinates. When properly scaled, load density p and/or bending strain κ may share the same axis as the position coordinates. For example, $Y(p \times 10^{-1})$ or $Y(p \times 10^{-1}, \kappa \times 10^{-2})$ means that $p \times 10^{-1}$ or $\kappa \times 10^{-2}$ share the same scale as position or displacement coordinate Y; 10 units of p and/or 100 units of κ equal 1 unit of Y.

For the *model order analysis*, instead of a standard analysis of variance (Miller [49], Bates and Watts [50]), the relative model order or relative number of the unknown variables is used and defined as the ratio of the number of the independent unknown load coefficients N_x to the number of measured data N_m:

$$N_m^x = \frac{N_x}{N_m} = \frac{N_{\text{elm}}(1 + \text{degree of IL polynomials})}{N_m} \tag{19}$$

When $N_m^x < 1$, the inverse problem is potentially overdetermined with a unique solution, but when $N_m^x > 1$, the inverse problem is underdetermined with nonuniqueness of the solutions. The extracted

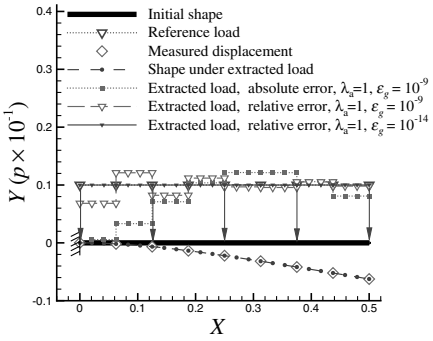

Fig. 3 Comparison of extracted loads for cantilever beam with absolute or relative error between calculated and measured displacements.

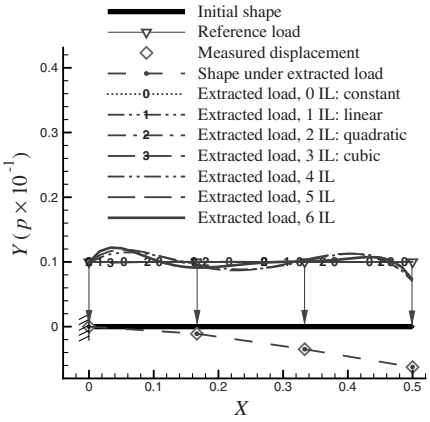

Fig. 4 Extracted load for cantilever beam subjected to uniform reference load as a function of number of integrated Legendre polynomials.

load error variance is defined as the average extracted load error over the beam length:

$$E_{\text{load}}^{\text{Ext}} = \frac{1}{L}\sum_{e=1}^{N_{\text{elm}}}\int_0^1 [p_{\text{ext}}^e(\xi) - p_{\text{ref}}^e(\xi)]^2 \mathrm{d}\xi \tag{20}$$

where p_{ext}^e and p_{ref}^e are extracted load density and reference applied load density over element e, respectively.

The basic studies are conducted for a planar uniform cantilever beam subjected to distributed load: the load density p has units of (EI/L^3); $L = 0.5$. Three kinds of load distribution of reference load will be studied: uniformly, linearly, and/or sinusoidally distributed.

A. Effect of Measurement Methods: Absolute Error and Relative Error

This example was used to compare the extracted loads obtained using two different displacement measurements. One was the absolute measurement and the other was the relative measurement. As shown in Fig. 3 and Table 1, the load updating problem remains *overdetermined* (the relative model order $N_m^x = N_x/N_m = 8/9$) though the nine measured displacement components are only taken at the two ends of the beam and seven joint points of the eight beam elements. It implies that there is a unique LSQ solution. The applied reference load was uniformly distributed and the extracted load within an element was also assumed to be uniformly distributed. Eight four-noded curved beam elements were used to model the beam. The extracted load with relative error of displacements was closer to the applied reference load than that with absolute error of displacements.

As seen in Fig. 3, when the absolute displacement a_i is used, the displacement error $a_i - a_{mi}$ and its gradient $a_{i,x}$ with respect to the load x close to the fixed end are smaller. This would make the load stop at a low-level x. When the relative displacement a_i/a_{mi} is used, however, its gradient $a_{i,x}/a_{mi}$ with respect to the load x is larger if a_{mi} is smaller. This would make the load stop at a higher level x/a_{mi}. It is concluded that calculating the error between the calculated and measured displacements in the relative sense [Eq. (8)] is better than in the absolute sense [Eq. (7)]. By increasing the accuracy from $\varepsilon_g = 1 \times 10^{-9}$ to $\varepsilon_g = 1 \times 10^{-14}$ (which is closer to the machine precision $\varepsilon_M = 2.22 \times 10^{-16}$), the extracted load agrees perfectly with the reference applied load.

In all the examples that follow, the relative measurement is used.

B. Effect of the Order of Integrated Legendre Polynomials

Because the extracted load within an element is represented by a linear combination of integrated Legendre polynomials, a numerical investigation was carried out on a single elemented cantilever beam of four nodes and four measured displacement components to see the effect of different orders of the polynomials on the extracted load for a uniformly distributed reference load, as shown in Fig. 4 and Table 2. The results show that when the order of polynomials is small enough as to make the problem determined or overdetermined, i.e., $N_m^x = N_x/N_m \leq 1$, the applied load can be better extracted. An increase in the order of polynomials does not always result in a better extracted load. Instead, a higher order of polynomials introduces more unknowns, and thus tends to make the problem underdetermined, and results in oscillating extracted loads.

C. Effect of Element Size

Refer to Fig. 5 and Table 3. The extracted loads for applied reference loads with uniform, linear, and sinusoidal distributions were investigated as functions of the number of elements used. The number of elements used was one, two, four, and eight, respectively. The extracted load within an element was assumed constant. In all the cases shown in the figure and table, the measured data were taken only at four points except for Fig. 5d. It appears that the problem is determined or overdetermined for all cases except for the case of eight elements and better extracted loads are expected. However, as the constant extracted loads of fewer elements cannot better represent the nonuniform load distributions, the extracted load errors tend to be dominant.

Therefore, an increase in the number of finite elements does not help in extracting a load closer to the reference load though it has a potential to better represent the nonuniform distribution of an applied

Table 1 $E_{\text{load}}^{\text{Ext}}$ vs absolute and relative displacement measurements

Measurement method	Absolute displacement	Relative displacement $\varepsilon_g = 1 \times 10^{-9}$	Relative displacement $\varepsilon_g = 1 \times 10^{-14}$
$N_m^x = N_x/N_m$	8/9	8/9	8/9
$E_{\text{load}}^{\text{Ext}}$	6.229×10^{-2}	2.219×10^{-2}	1.225×10^{-10}

Table 2 $E_{\text{load}}^{\text{Ext}}$ vs the degree of integrated Legendre polynomial within one element

Degree of IL	0	1	2	3	4	5	6
$N_m^x = N_x/N_m$	1/4	2/4	3/4	4/4	5/4	6/4	7/4
$E_{\text{load}}^{\text{Ext}}$, uniform load	0.000	0.000	0.000	8.864×10^{-4}	1.436×10^{-2}	1.565×10^{-2}	1.294×10^{-2}

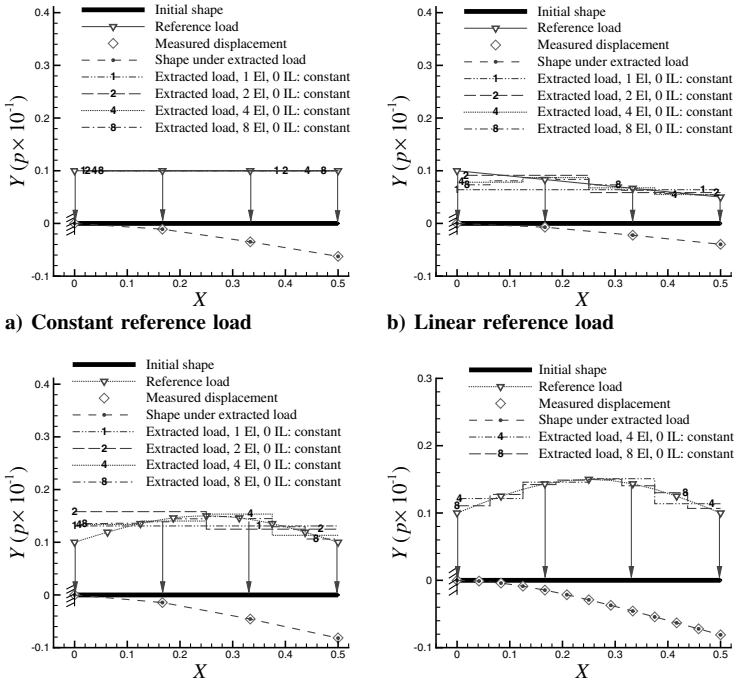

a) Constant reference load

b) Linear reference load

c) Sinusoidal reference load

d) Sinusoidal reference load (13 measured points for displacements)

Fig. 5 Extracted load for a cantilever beam as a function of number of elements.

load. Instead, the minimum number of elements that meets the requirement of the accuracy of FEA may get the extracted load closest to the reference load for a given number and distribution of measured points over the beam. This makes using a high precision four-noded beam element advantageous because one can use fewer elements to obtain a regularization effect by turning the problem to be an overdetermined one.

Increasing the number of elements seemingly tends to improve the quality of the extracted load far off the supporting boundaries. In fact, the better extracted load was obtained more due to a better representation of the load distribution. The extracted load got worse near the boundaries as the number of elements increased due to the limited number of the measured points. This conclusion is seemingly contrary to the previous observation that aimed at reducing the boundary effect (Johnson [38], Chock and Kapania [3]) by increasing the number of elements near the boundaries. In fact, the reduced boundary effect was more due to an increase in the *noise-free* measured data (and reduced model order) near the boundaries. Compare Figs. 5c and 5d.

D. Effect of Density of Measured Points

Generally speaking, the more information about the structural model, load, and response is known, the better the extracted load tends to be. Therefore, we expect that an increase of the local and global density of noise-free, sparsely measured points does help in bringing the extracted load closer to the reference load (under which the measured data are taken).

The extracted loads for the uniformly, linearly, and sinusoidally distributed reference loads, respectively, with constant extracted load within an element are presented as functions of the number of measured points in Fig. 6 and Table 4 (for linear reference load), in which eight elements were used and the number of measured points is four, seven, 13, and 25, respectively. The load within each of the elements was assumed to be uniformly distributed. Obviously, more measured points tend to improve the quality of the extracted load, especially near the boundaries, without increasing the number of elements, which tends to reduce the problem to be overdetermined or more overdetermined ($N_m^x < 1$).

It should be understood that when the number of measured data is too large, the accuracy of the extracted load will deteriorate due to the truncated error of the limited computer precision. Therefore, if the actual measured data are continuously scanned, and only those data at the FEM nodes should be used.

E. Effect of Enforcing Smoothing and C^0 Continuity

When a polynomial of higher order is assumed within an element for extracting a load, the resulting extracted load will have unexpected oscillation within an element and discontinuity between two adjacent elements. Therefore, it may be useful to enforce C^0 continuity and load smoothing. The illustrative example was a planar uniform cantilever beam subjected to linearly distributed load. Refer to Fig. 7. The applied reference load was linearly distributed but a linear combination of the first four integrated Legendre polynomials (highest degree is three) was used to represent the load distribution over an element for load extraction. Eight four-noded beam elements ($N_{\text{elm}} = 8$) were used. The $N_m = 25$ measured displacement components were taken from all of the available nodes ($N_{\text{node}} = 3N_{\text{elm}} + 1 = 25$). The first four integrated Legendre polynomials were used for the extracted load representation within an element. Therefore, the problem is underdetermined at the beginning as the relative model order $N_m^x = N_x/N_m = 8 \times (1 + 3)/25 = 32/25 > 1$. When only the C^0 continuity is

Table 3 $E_{\text{load}}^{\text{Ext}}$ vs the number of elements, N_{elm}

N_{elm}	1	2	4	8
$N_m^x = N_x/N_m$	1/4	2/4	4/4	8/4
$E_{\text{load}}^{\text{Ext}}$, uniform load	0.000	0.000	0.000	0.000
$E_{\text{load}}^{\text{Ext}}$, linear load	2.575×10^{-2}	1.187×10^{-2}	1.300×10^{-2}	1.357×10^{-2}
$E_{\text{load}}^{\text{Ext}}$, sine load	2.190×10^{-2}	3.501×10^{-2}	1.771×10^{-2}	1.532×10^{-2}

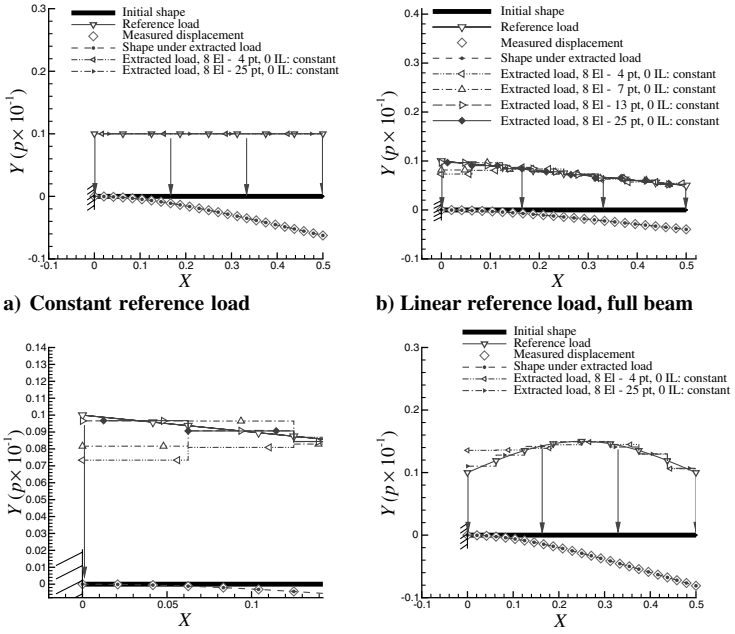

a) Constant reference load

b) Linear reference load, full beam

c) Linear reference load, closeup at fixed end

d) Sinusoidal reference load

Fig. 6 Extracted load for a cantilever beam as a function of number of measured points.

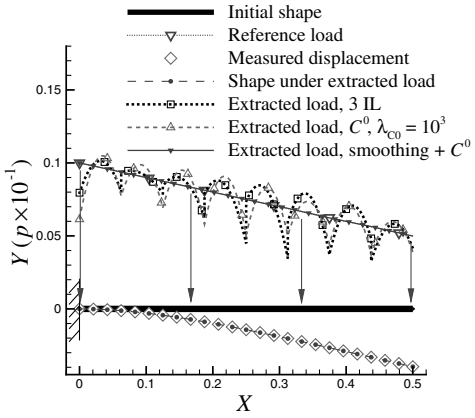

Fig. 7 Constraining the extracted load through load smoothing within an element and C^0 between two adjacent elements: λ_S, $\lambda_{C^0} = 1 \times 10^3$ continuity.

enforced, it equivalently adds $N_{\text{elm}} - 1 = 7$ constraints to the model. This only brings the model to appear barely determined $N_m^x = (32 - 7)/25 = 1$. Although the load discontinuity disappears, the extracted load oscillation still exists. It implies that the problem remains ill-posed. When both the C^0 continuity and load smoothing are enforced, it equivalently adds $N_{\text{elm}} - 1 + N_{\text{elm}} = 15$ constraints to the model. This brings the model to appear overdetermined $N_m^x = (32 - 15)/25 = 17/25 < 1$. Both the load discontinuity and oscillation disappear!

It should be pointed out that this example illustrates that both the C^0 continuity and load smoothing are special or variant cases of generalized Tikhonov regularization technique [Eqs. (15–18)] that by enforcing constraints on loads the oscillations in extracted loads due to undeterminedness of the system can be smoothed out. That is, enforcing constraints by a priori knowledge helps changing the inverse problem from an underdetermined system to a determined or overdetermined one.

On the other hand, the undeterminedness of the system in this example is purely due to the fact that extra unknowns are introduced using higher order of polynomials to parameterize the applied load. This should point us to another direction to obtain a determined or overdetermined model by reducing the number of unknown load parameters. This can be realized by either using lower order polynomials within an element to represent the applied load or parameterize the applied load distribution across-elementwise or globally using less unknown load parameters.

In this study, however, we address using lower order of polynomials within a higher-order element for applied load representation. This works well benefiting from the fact that we use a high-precisioned, four-noded, cubic beam element. This makes it possible that for a given and limited number of sparsely measured data, fewer elements of higher order and load representation of lower polynomials can be used. All the examples that follow are set up according to this guideline.

F. Application to a Portal Frame

After the basic studies on the load updating for finite element models were performed for a cantilever beam using the four-noded beam element, the proposed approach and recommendations were applied to extract loads acting on a portal frame with a height of unit length and a span of two units. The load density p has units of EI/h^3 where h is the height of the frame. Note that both the applied load and deformation are out of plane. One element was used for each of the two columns (under linearly distributed reference load with one unit of load at one end and 0.5 at the other end) and two elements were used for the top beam (under sinusoidally distributed reference load with zero mean value and amplitude of 0.5 unit). For load updating, quadratically distributed load was assumed to be acting on each element. Therefore, the relative model order $N_m^x = N_x/N_m = 4 \times (1 + 2)/13 = 12/13 < 1$, which means it is an overdetermined

Table 4 $E_{\text{load}}^{\text{Ext}}$ vs the number of measured points, N_m.

N_m	4	7	13	25
$N_m^x = N_x/N_m$	8/4	8/7	8/13	8/25
$E_{\text{load}}^{\text{Ext}}$, linear load	1.357×10^{-2}	8.766×10^{-3}	2.706×10^{-3}	2.705×10^{-3}

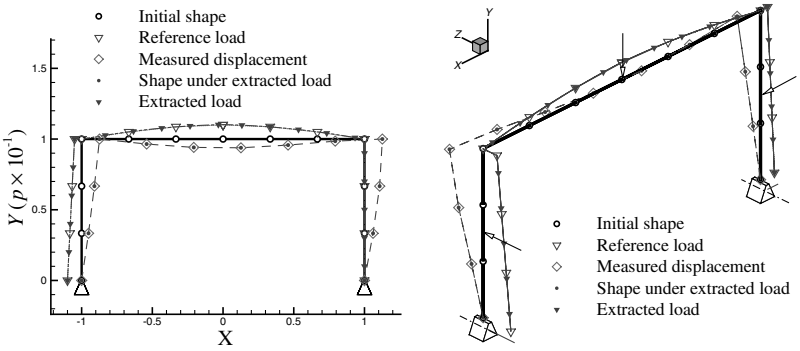

a) Two-dimensional view **b) Three-dimensional view**

Fig. 8 Extracting in-plane and out-plane loads for a portal frame.

problem. The results in Fig. 8 show that the extracted load agreed well with the applied reference load. (The applied load directions are shown in Fig. 8b.)

G. Application to Highly Oscillating Load Updating

It is interesting to see the performance of the load updating for FEM under *non-noisy* but highly varying load. The example being investigated was a planar uniform cantilever or simply supported beam subjected to sinusoidally distributed load; the load density p has units of EI/L^3, $L = 0.5$.

For all the cases shown in Fig. 9, a constant extracted load was assumed for each four-noded beam element and the measured displacement components were taken at all available nodes. As a large number of elements was used, the relative model order was $N_m^x \approx 1/3 < 1$. It means the problem is very overdetermined.

The applied reference load (RL) was sinusoidally distributed with unit mean value. The extracted load (EL) was assumed uniformly distributed within an element. In Fig. 9a, the EL agreed well with the RL. Fig. 9b shows that the EL agreed well with the RL at the first three sine waves near the fixed end but tended to be close to the unit mean value of the RL at the other three sine waves near the free end. In Fig. 9c, the EL agreed well with the RL at only 1.5 sine waves near the fixed end but tended to be close to the unit mean value of the RL near the free end. Results using both 120 and 240 elements are almost identical.

The results for the cantilever beam show that the load updating using the four-noded cubic beam element is able to extract the applied load for moderately oscillating load (where using element of lower order may fail), but is only good to extract the mean value of the highly oscillating load.

In other words, the load updating as a typical inverse problem tends to extract the average part of the applied load but filters out the highly oscillating part of the load. This numerical "damping" effect may contribute to truncated errors due to the limited machine precision. Figure 9 shows the results for the cantilever beam.

H. Measured Strains Based Load Updating

A planar uniform cantilever beam is subjected to distributed load; the load density p has units of EI/L^3, $L = 0.5$. The measured data were the bending strains taken at three Gaussian points of each of the eight four-noded beam elements. Therefore, the relative model order was $N_m^x = 8/(8 \times 3) = 1/3 < 1$, implying an overdetermined problem. The sensitivities of the strains with respect to the assumed load coefficients were calculated according to the method explained in Appendix D. Whereas the uniformly distributed load was assumed within a single element, the applied reference load was uniformly, linearly, and sinusoidally distributed, respectively, as shown in Fig. 10. The results show that the extracted load agreed well with the applied load.

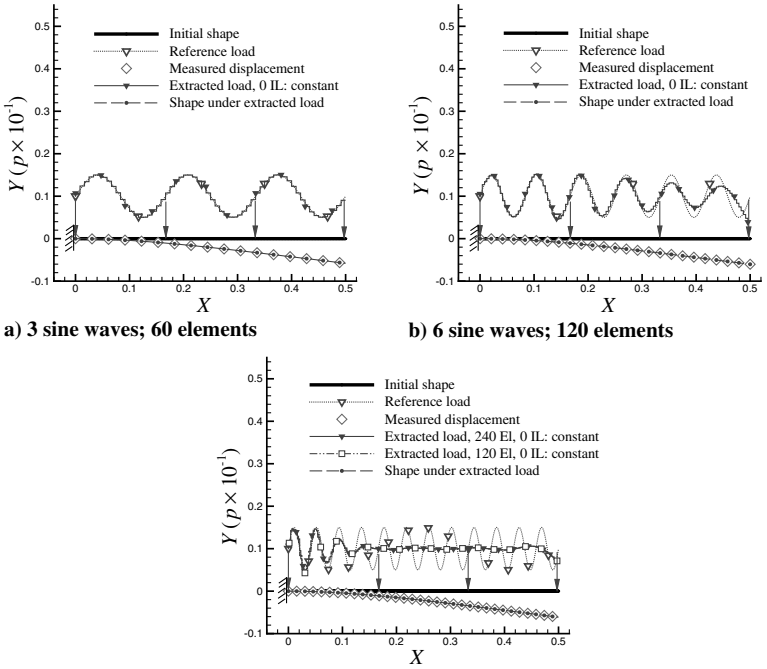

a) 3 sine waves; 60 elements **b) 6 sine waves; 120 elements**

c) 12 sine waves/unit mean value; 240 (120) elements

Fig. 9 Extracting highly oscillating load for a cantilever beam.

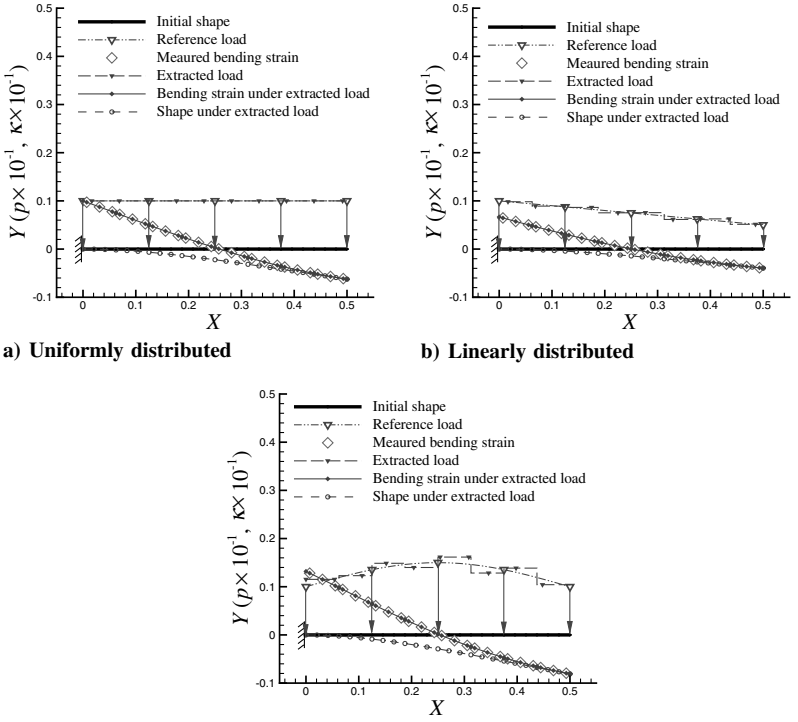

a) Uniformly distributed b) Linearly distributed

c) Sinusoidally distributed

Fig. 10 Extracting loads of different distributions for a cantilever beam.

I. Application to Geometrically Nonlinear Beam

Thus far, we have extracted loads acting on beams and frames assuming that the beam or the frame behaves linearly. The approach was also used to extract loads under which the response can be nonlinear. The finite element used in this study is capable of simulating geometrically nonlinear behavior. The capability to extract loads that lead to a nonlinear behavior was investigated for a cantilever beam subjected to self-weight, snow load, and pressure load. For nonlinear behavior, the axial displacement of the beam cannot be ignored, whereas it is ignored for a linear case. It should, however, be pointed out that it would be rather difficult to measure the axial displacement. Therefore, we investigated the role of measuring the axial displacement along with the transverse displacement.

The example being investigated was a planar uniform cantilever beam subjected to uniformly distributed load; the load density $p = 5$ has units of EI/L^3, $L = 0.5$.

In all cases, a uniform extracted load was assumed for each of eight four-noded beam elements. The measured displacements were taken from all 25 nodes. The problem was overdetermined for all cases as the relative model order $N_m^x \leq 8/(8 \times 3 + 1) \approx 1/3 < 1$. The full Newton–Raphson approach (Kapania and Li [42]) with 10 equal load steps was used to solve the geometrically nonlinear problem.

1. *Self-Weight Load*

For a self-weight-type load, the extracted load agrees well with the reference applied load when transverse displacement alone is taken as measured data, which is as good as when both transverse and axial displacement are used [see Fig. 11]. Fig. 11a shows that the applied load was extracted using transverse displacements only (the unknown axial displacements are set to zero in the figure) of all the 25 nodes. The extraction required 45.59 s of CPU time, 28 nonlinear finite element analyses, and 21 load updating iterations, stopping when the design step size was 0.00019. In Fig. 11b, the applied load was extracted using both transverse and axial displacement components of all the 25 nodes. The extraction required 45.58 s of CPU time, 15 nonlinear FEA, and 11 load updating iterations, stopping when the design step size was 0.00063.

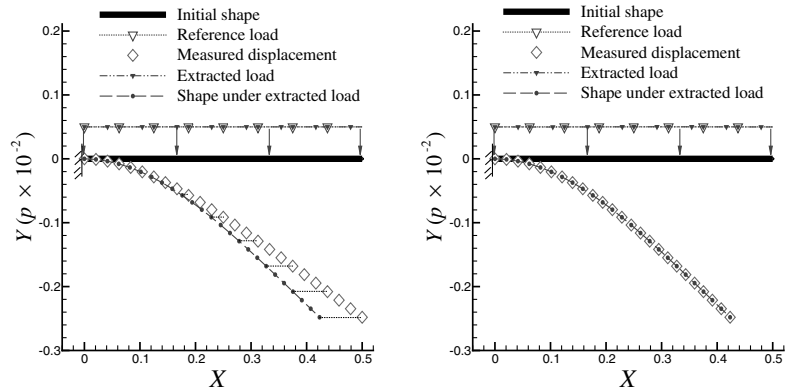

a) Transverse displacements only b) Transverse and axial displacements

Fig. 11 Extracting uniform self-weight type load for a cantilever beam. Eight finite elements were used to model the beam.

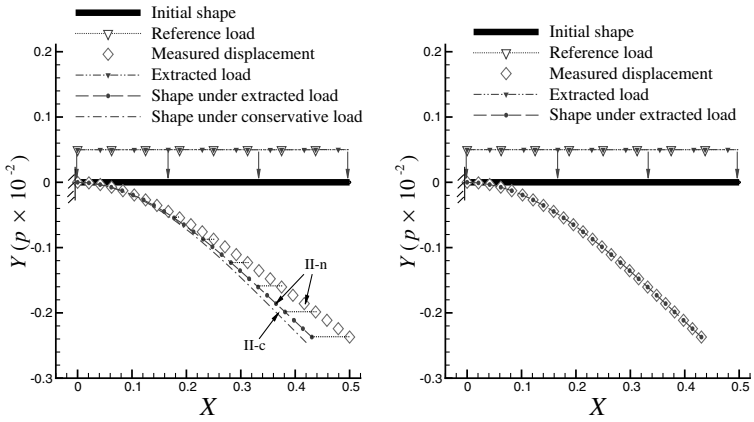

a) Transverse displacements only **b) Transverse and axial displacements**

Fig. 12 Extracting uniform snow loads of nonconservative consideration as compared with conservative consideration for a cantilever beam.

2. Snow Load

For a snow-type load [nonconservative consideration (type II-n) as compared with conservative consideration (type II-c)] (Kapania and Li [43]), the extracted load agrees well also with the reference applied load when transverse displacement alone is taken as the measured data, which is as good as when both transverse and axial displacement are used (Fig. 12). Eight finite elements were used to model the beam. Fig. 12a shows that the applied load was extracted using transverse displacements only (the unknown axial displacements are set to zero in the figure) of all the 25 nodes. The extraction required 57.30 s of CPU time, 23 nonlinear FEA, and 17 load updating iterations, stopping when the design step size was 0.00045. In Fig. 12b, the applied load was extracted using both transverse and axial displacement components of all the 25 nodes. The extraction required 44.26 s of CPU time, 16 nonlinear FEA, and 12 load updating iterations (LUI), stopping when the design stepsize was 0.0006.

3. Pressure Load

For a pressure type load, we found that when only transverse displacement (TD) was taken as the measured data, the load updating procedure failed to converge to a satisfactory solution for the given load level (Fig. 13a). The RL (very small in the figure) failed to be extracted using TD only. It stopped when the design stepsize (DS) was 1.114×10^{-12} but the objective did not converge to zero though each nonlinear FEA converged. However, simply adding an axial measured displacement at the free end (Fig. 13b), the extraction not only converged to the expected solution, but the extracted results are also as good as when both the transverse and axial displacements at all the 25 points are taken as the measured data (Fig. 13c). In Fig. 13b, the RL was extracted using TD and axial displacement (AD) measured only at the free-end. It took 28.98 s of CPU time, 18 FEA, and 14 LUI, stopping when DS was 0.00079. Fig. 13c shows that the RL was extracted using all TD and AD. It took 32.96 s of CPU time, 20 FEA, and 12 LUI, stopping when DS was 0.00065. Eight finite elements were used. The unknown axial displacements are set to zero in the figure.

IV. Conclusions

The load updating for geometrically linear and nonlinear beams/frames with the given noise-free measured deformation has been studied by the use of a four-noded curved beam element and the optimizer L-BFGS-B.

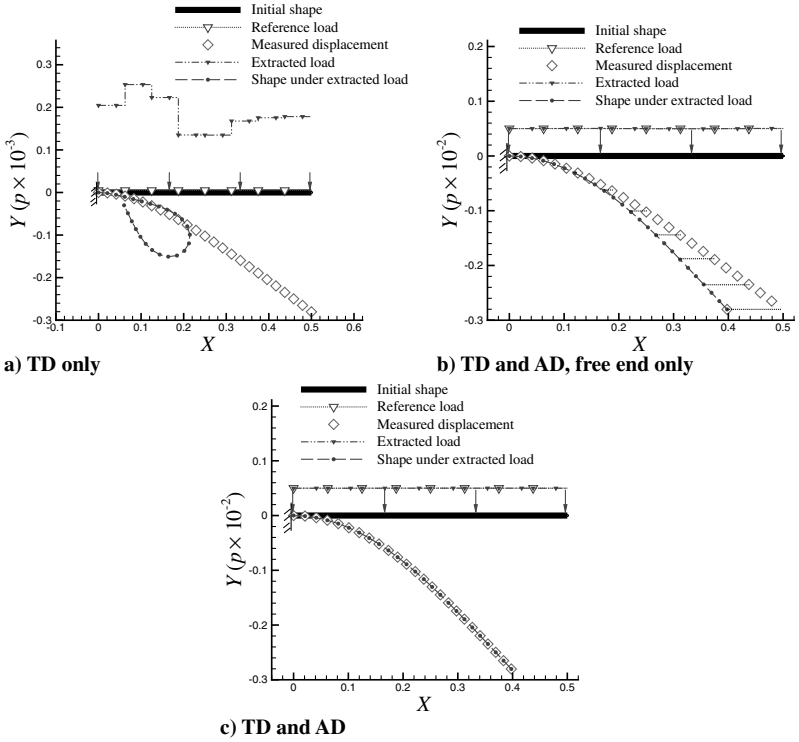

a) TD only **b) TD and AD, free end only**

c) TD and AD

Fig. 13 Extracting uniform pressure load for a cantilever beam with different choices of displacement measurements.

For the basic studies, the extracted load was represented within an element by a linear combination of integrated Legendre polynomials, the coefficients of which were taken as design variables of the least-squares problem.

Through a relative model order analysis, the benefits for solving load updating problems using the relative deformation measurement, the polynomials of lower orders, the elements of larger sizes (because of using the high-precision four-noded beam element), and the denser sparsely measured points were studied for linear responses under the applied loads of different types.

It was confirmed that using the reduced number of unknown variables to obtain an overdetermined inverse problem helps get unique and stable extracted loads. Though this conclusion was verified mainly through illustrative examples for a cantilever beam, it was generally applicable to other load updating or inverse problems.

Application examples were given for a three-dimensional portal frame load updating, extracting highly oscillating loads, and a strain-based cantilever beam load updating, and load updating for geometrically nonlinear finite element models under self-weight, snow, and/or pressure loads.

The extraction of highly varying applied load shows that the load updating for FEM using the four-noded beam element is able to extract moderate waved load, but only extract the average part of the load and filter off the highly oscillating part. This damping effect is due to the truncated error of numerical implementation.

For a linear FEM, using only transverse components of the displacements are enough to extract the applied load of a cantilever beam or simply-supported beam. However, for a geometrically nonlinear FEM, both transverse and axial components of the displacement at the measured points have to be used for a higher load level, especially for pressure load.

Present conclusions may be applied to the measurement-based load updating for general finite element models when the measured data are presmoothed or the noise in the data is prefiltered off.

Appendix A: Legendre Polynomials

Let $\alpha = 0, 1, \ldots, N_c^e$

$$L_\alpha(x) \equiv \frac{1}{2^\alpha \alpha!}\frac{d^\alpha}{dx^\alpha}(x^2-1)^\alpha \tag{A1}$$

be the αth Legendre polynomial, and

$$\tilde{L}_\alpha(x) \equiv \gamma_\alpha \int_{-1}^{x} L_\alpha(x)\,\mathrm{d}x \quad \text{for } \alpha \geq 2 \tag{A2}$$

be the αth integrated Legendre polynomial with

$$\gamma_\alpha = \sqrt{\frac{(2\alpha-3)(2\alpha-1)(2\alpha+1)}{4}} \tag{A3}$$

By definition,

$$\tilde{L}_0(x) = \frac{1+x}{2} \qquad \tilde{L}_1(x) = \frac{1-x}{2} \tag{A4}$$

The properties

$$L_\alpha(x) = \frac{2\alpha-1}{\alpha}xL_{\alpha-1}(x) - \frac{\alpha-1}{\alpha}L_{\alpha-2}(x)$$

$$[L_0(x)=1, \quad L_1(x)=x] \qquad \int_{-1}^{1} L_\alpha(x)L_\beta(x)\,\mathrm{d}x = \delta_{\alpha\beta}\frac{2}{2\alpha+1}$$

$$\tilde{L}_\alpha(x) = \sqrt{\frac{(2\alpha+1)(2\alpha-3)}{4(2\alpha-1)}}[L_\alpha(x) - L_{\alpha-2}(x)] \qquad \tilde{L}_\alpha(-1) = 0$$

$$\tilde{L}_\alpha(1) = 0 \tag{A5}$$

are true for $\alpha \geq 2$.

In the integral, all powers lower than n of the Legendre polynomial yield zero when integrated against the cosine (because of the orthogonality of the cosines).

Let $\alpha = 0, 1, \ldots, N_c^e$

$$L_\alpha(x) \equiv \frac{1}{2^\alpha \alpha!}\frac{d^\alpha}{dx^\alpha}(x^2-1)^\alpha \tag{A6}$$

the αth Legendre polynomial,

$$\tilde{L}_\alpha(x) \equiv \gamma_\alpha \int_{-1}^{x} L_\alpha(x)\,\mathrm{d}x \quad \text{for } \alpha \geq 2 \tag{A7}$$

the αth integrated Legendre polynomial with

$$\gamma_\alpha = \sqrt{\frac{(2\alpha-3)(2\alpha-1)(2\alpha+1)}{4}} \tag{A8}$$

By definition,

$$\tilde{L}_0(x) = \frac{1+x}{2} \qquad \tilde{L}_1(x) = \frac{1-x}{2} \tag{A9}$$

The properties

$$L_\alpha(x) = \frac{2\alpha-1}{\alpha}xL_{\alpha-1}(x) - \frac{\alpha-1}{\alpha}L_{\alpha-2}(x)$$

$$[L_0(x)=1, \quad L_1(x)=x] \qquad \int_{-1}^{1} L_\alpha(x)L_\beta(x)\,\mathrm{d}x = \delta_{\alpha\beta}\frac{2}{2\alpha+1}$$

$$\tilde{L}_\alpha(x) = \sqrt{\frac{(2\alpha+1)(2\alpha-3)}{4(2\alpha-1)}}[L_\alpha(x) - L_{\alpha-2}(x)] \qquad \tilde{L}_\alpha(-1) = 0$$

$$\tilde{L}_\alpha(1) = 0 \tag{A10}$$

are true for $\alpha \geq 2$.

In the integral, all powers lower than n of the Legendre polynomial yield zero when integrated against the cosine (because of the orthogonality of the cosines).

Appendix B: Force Coefficient Matrix in Element Level

In general, for our geometrically nonlinear FEM for the three-dimensional case, we can start with the state equation of a nonlinear structural system (Kapania and Li [43]):

$$\boldsymbol{R}(\boldsymbol{a}, \boldsymbol{c}, \lambda) = \boldsymbol{q}_{\text{int}}(\boldsymbol{a}) - \lambda \boldsymbol{q}_{\text{ext0}}(\boldsymbol{a}, \boldsymbol{c}) = 0 \tag{B1}$$

where $\boldsymbol{R}$ is the residual vector, $\boldsymbol{q}_{\text{int}}$ is the nodal internal force vector, $\boldsymbol{q}_{\text{ext0}}$is the nodal external load vector calculated at the applied load level, λ is the proportional nodal loading factor, $\boldsymbol{a} = \boldsymbol{a}(\boldsymbol{c}, \lambda)$ is the nodal displacement vector, and $\boldsymbol{c}$ is the load (force) coefficient vector; $\boldsymbol{q}_{\text{int}}$ and $\boldsymbol{q}_{\text{ext0}}$ are summed from the nodal internal and external load vectors contributed by an element $e \in [1, N_{\text{elm}}]$:

$$\boldsymbol{q}^e_{\text{int}} = \begin{bmatrix} \boldsymbol{q}^e_{\text{int1}} \\ \vdots \\ \boldsymbol{q}^e_{\text{int}I^e_{\text{node}}} \\ \vdots \\ \boldsymbol{q}^e_{\text{int}N^e_{\text{node}}} \end{bmatrix} \quad \text{and} \quad \boldsymbol{q}^e_{\text{ext0}} = \begin{bmatrix} \boldsymbol{q}^e_{\text{ext01}} \\ \vdots \\ \boldsymbol{q}^e_{\text{ext0}I^e_{\text{node}}} \\ \vdots \\ \boldsymbol{q}^e_{\text{ext0}N^e_{\text{node}}} \end{bmatrix} \tag{B2}$$

respectively, where

$$\boldsymbol{q}^e_{\text{int}I^e_{\text{node}}} = \begin{bmatrix} \boldsymbol{P}^e_{\text{int}I^e_{\text{node}}} \\ \boldsymbol{M}^e_{\text{int}I^e_{\text{node}}} \end{bmatrix} \tag{B3}$$

where

$$\boldsymbol{P}^e_{\text{int}I^e_{\text{node}}} = \int_0^1 N_{I^e_{\text{node}},\xi}\boldsymbol{n}^e\,\mathrm{d}\xi \tag{B4}$$

and

$$\boldsymbol{M}^{e}_{\text{int}I^e_{\text{node}}} = \int_0^1 (N_{I^e_{\text{node}},\xi}\boldsymbol{m}^e - N_{I^e_{\text{node}}}\hat{\boldsymbol{\varphi}}^e_{,\xi}\boldsymbol{n}^e)\,\mathrm{d}\xi \tag{B5}$$

are the nodal internal force and moment vectors at node I^e_{node} contributed by element e, respectively, and

$$\boldsymbol{q}^{e}_{\text{ext0}I^e_{\text{node}}} = \begin{bmatrix} \boldsymbol{P}^e_{\text{ext0}I^e_{\text{node}}} \\ \boldsymbol{M}^e_{\text{ext0}I^e_{\text{node}}} \end{bmatrix} \tag{B6}$$

where

$$\begin{aligned}\boldsymbol{P}^e_{\text{ext0}I^e_{\text{node}}} &= \int_0^1 N_{I^e_{\text{node}}}[\boldsymbol{\mathcal{N}}^e_g + \boldsymbol{\mathcal{N}}^e_d \sin(\boldsymbol{d}^e, \boldsymbol{\varphi}^e_{0,s}) + \boldsymbol{\Lambda}^e\bar{\boldsymbol{\mathcal{N}}}^e_p]\mathcal{J}^e\,\mathrm{d}\xi \\ &= \int_0^1 N_{I^e_{\text{node}}}[\boldsymbol{\mathcal{N}}^e_g + \boldsymbol{\mathcal{N}}^e_d \sin(\boldsymbol{d}^e, \boldsymbol{\varphi}^e_{0,s}) + \boldsymbol{\mathcal{N}}^e_p]\mathcal{J}^e\,\mathrm{d}\xi\end{aligned} \tag{B7}$$

and

$$\boldsymbol{M}^{e}_{\text{ext}I^e_{\text{node}}} = 0 \tag{B8}$$

are the nodal external force and zero moment vectors at node I^e_{node} contributed by the distributed force acting on element e at the applied load level, respectively.

Assume that

$$\boldsymbol{\mathcal{N}}^{e}_{l} = \boldsymbol{c}^{le}_{\alpha} P_\alpha(\xi_1) \tag{B9}$$

where P_α are the basis functions, taken to be the integrated Legendre polynomials, $\alpha = 1, 2, \ldots, N^e_c$ (summation convention holds for α) with N^e_c as the number of basis functions considered for each element, and $\boldsymbol{c}^{le}_\alpha$ are the load (force) coefficient vectors for each element, and the subscript $l = g, d, p$ identifies the load type, i.e., the self-weight load, snow load, and pressure load, respectively, (for $l = p$, the material form $\bar{\boldsymbol{\mathcal{N}}}^e_p$ is used instead of the spatial form $\boldsymbol{\mathcal{N}}^e_p$).

Now let us consider the dependency of the three components of the force coefficient vector, e.g., $\boldsymbol{c}^{le}_\alpha$. We know from Eq. (B9) that $\boldsymbol{c}^{le}_\alpha$ determine both the direction and the amplitude of the external force distribution over an element. We consider three cases:

1) The one-dimensional case, i.e., the direction of $\boldsymbol{c}^{le}_\alpha$ is given over the element by the vector $\boldsymbol{d}^{le}_1$:

$$\boldsymbol{c}^{le}_{\alpha} = x^{le}_{1\alpha}\boldsymbol{d}^{le}_1 \tag{B10}$$

2) The two-dimensional case, i.e., the plane of $\boldsymbol{c}^{le}_\alpha$ is same over all α and given by the vectors $\boldsymbol{d}^{le}_1$ and $\boldsymbol{d}^{le}_2$:

$$\boldsymbol{c}^{le}_{\alpha} = x^{le}_{1\alpha}\boldsymbol{d}^{le}_1 + x^{le}_{2\alpha}\boldsymbol{d}^{le}_2 \tag{B11}$$

3) The more general three-dimensional case, i.e., the direction of $\boldsymbol{c}^{le}_{N\alpha}$ is unknown:

$$\boldsymbol{c}^{le}_{\alpha} = x^{le}_{1\alpha}\boldsymbol{d}^{l}_1 + x^{le}_{2\alpha}\boldsymbol{d}^{l}_2 + x^{le}_{3\alpha}\boldsymbol{d}^{l}_3 \tag{B12}$$

where $\boldsymbol{d}^l_i = \boldsymbol{e}_i$ for $l = g, d$ (self-weight load and snow load), and $\boldsymbol{d}^l_i = \boldsymbol{t}_i$ for $l = p$ (pressure load).

Collectively, we can combine the three cases into one form:

$$\mathbf{c}^{le}_{\alpha} = \mathbf{D}^{le}\mathbf{x}^{le}_{\alpha} \tag{B13}$$

where $\mathbf{x}^{le}_\alpha$ are called independent force coefficient vectors.

Therefore,

$$\begin{aligned}\boldsymbol{P}^{e}_{\text{ext0}I^e_{\text{node}}} = \int_0^1 N_{I^e_{\text{node}}}[&\boldsymbol{c}^{ge}_\alpha P_\alpha(\xi_1) + \boldsymbol{c}^{de}_\alpha P_\alpha(\xi_1)\sin(\boldsymbol{d}^e, \boldsymbol{\varphi}^e_{0,s}) \\ &+ \boldsymbol{\Lambda}^e\boldsymbol{c}^{pe}_\alpha P_\alpha\xi_1)]\mathcal{J}^e\,\mathrm{d}\xi\end{aligned} \tag{B14}$$

The variations with respect to load (force) coefficient vectors

$$\delta_c\boldsymbol{P}^e_{\text{ext0}I^e_{\text{node}}} = \boldsymbol{F}^{ge}_{cI^e_{\text{node}}\alpha}\delta\boldsymbol{c}^{ge}_\alpha + \boldsymbol{F}^{de}_{cI^e_{\text{node}}\alpha}\delta\boldsymbol{c}^{de}_\alpha + \boldsymbol{F}^{pe}_{cI^e_{\text{node}}\alpha}\delta\boldsymbol{c}^{pe}_\alpha \tag{B15}$$

where, noticing that $\boldsymbol{I}_3$ denotes the identity tensor of order two,

$$\begin{aligned}\boldsymbol{F}^{ge}_{cI^e_{\text{node}}\alpha} &= \int_0^1 \boldsymbol{I}_3 N_{I^e_{\text{node}}} P_\alpha(\xi_1)\mathcal{J}^e\,\mathrm{d}\xi \\ \boldsymbol{F}^{de}_{cI^e_{\text{node}}\alpha} &= \int_0^1 \boldsymbol{I}_3 N_{I^e_{\text{node}}} P_\alpha(\xi_1)\sin(\boldsymbol{d}^e, \boldsymbol{\varphi}^e_{0,s})\mathcal{J}^e\,\mathrm{d}\xi \\ \boldsymbol{F}^{pe}_{cI^e_{\text{node}}\alpha} &= \int_0^1 \boldsymbol{\Lambda}^e N_{I^e_{\text{node}}} P_\alpha(\xi_1)\mathcal{J}^e\,\mathrm{d}\xi\end{aligned} \tag{B16}$$

For a single node of an element,

$$\delta_c\boldsymbol{q}^e_{\text{ext0}I^e_{\text{node}}} = \tilde{\boldsymbol{F}}^{ge}_{cI^e_{\text{node}}\alpha}\delta\boldsymbol{c}^{ge}_\alpha + \tilde{\boldsymbol{F}}^{de}_{cI^e_{\text{node}}\alpha}\delta\boldsymbol{c}^{de}_\alpha + \tilde{\boldsymbol{F}}^{pe}_{cI^e_{\text{node}}\alpha}\delta\boldsymbol{c}^{pe}_\alpha \tag{B17}$$

where

$$\tilde{\boldsymbol{F}}^{le}_{cI^e_{\text{node}}\alpha} = \begin{bmatrix} \boldsymbol{F}^{le}_{cI^e_{\text{node}}\alpha} \\ 0 \end{bmatrix} \tag{B18}$$

For a single element e with N^e_{node} nodes contributed by load type l, noticing Eq. (B13),

$$\delta_c\boldsymbol{q}^{le}_{\text{ext0}} = \tilde{\boldsymbol{F}}^{le}_c\delta\boldsymbol{c}^{le} = \tilde{\boldsymbol{F}}^{le}_{c\alpha}\delta\boldsymbol{c}^{le}_\alpha \tag{B19}$$

$$\delta_x\boldsymbol{q}^{le}_{\text{ext0}} = \tilde{\boldsymbol{F}}^{le}_x\delta\boldsymbol{x}^{le} = \tilde{\boldsymbol{F}}^{le}_{x\alpha}\delta\boldsymbol{x}^{le}_\alpha = \tilde{\boldsymbol{F}}^{le}_{c\alpha}\boldsymbol{D}^{le}\delta\boldsymbol{x}^{le}_\alpha \tag{B20}$$

where

$$\begin{aligned}&\tilde{\boldsymbol{F}}^{le}_x = \begin{bmatrix} \tilde{\boldsymbol{F}}^{le}_{x1} & \cdots & \tilde{\boldsymbol{F}}^{le}_{xN_c} \end{bmatrix}, \qquad \tilde{\boldsymbol{F}}^{le}_{x\alpha} = \tilde{\boldsymbol{F}}^{le}_{c\alpha}\boldsymbol{D}^{le} \\ &\tilde{\boldsymbol{F}}^{le}_{c\alpha} = \begin{bmatrix} \tilde{\boldsymbol{F}}^{le}_{c1\alpha} \\ \vdots \\ \tilde{\boldsymbol{F}}^{le}_{cN^e_{\text{node}}\alpha} \end{bmatrix}, \quad \text{and} \quad \delta\boldsymbol{x}^{le} = \begin{bmatrix} \delta\boldsymbol{x}^{le}_1 \\ \vdots \\ \delta\boldsymbol{x}^{le}_{N^e_c} \end{bmatrix}\end{aligned} \tag{B21}$$

Appendix C: Derivatives of Displacements with Respect to Load (Force) Coefficient Vector

In the *linearized* incremental form, the state equation can be written as

$$R + \Delta R = 0 \tag{C1}$$

and

$$\Delta R = \Delta_a R + \Delta_x R + \Delta_\lambda R = R_{,\boldsymbol{a}}\Delta\boldsymbol{a} + R_{,\boldsymbol{x}}\Delta\boldsymbol{x} + R_{,\lambda}\Delta\lambda \tag{C2}$$

where the linearized increment operator Δ has been decomposed into three parts: the linearized increment Δ_a due to a change in $\boldsymbol{a}$, linearized increment Δ_x (or Δ_c) due to a change in $\boldsymbol{x}$ (or $\boldsymbol{c}$), and linearized increment Δ_λ due to a change in λ. The Jacobians $R_{,\boldsymbol{a}}$, $R_{,\boldsymbol{x}}$, and $R_{,\lambda}$ are the *partial* derivatives of the residual R with respect to the state vector $\boldsymbol{a}$, load design vector $\boldsymbol{x}$, and load factor λ, respectively:

$$R_{,\boldsymbol{a}} = R_{,\boldsymbol{a}}(\boldsymbol{a}, \boldsymbol{x}, \lambda) = \boldsymbol{q}_{\text{int},\boldsymbol{a}} - \lambda\boldsymbol{q}_{\text{ext0},\boldsymbol{a}} \tag{C3}$$

$$R_{,\boldsymbol{c}} = R_{,\boldsymbol{x}}(\boldsymbol{a}, \boldsymbol{x}, \lambda) = \boldsymbol{q}_{\text{int},\boldsymbol{x}} - \lambda\boldsymbol{q}_{\text{ext0},\boldsymbol{x}} = -\lambda\boldsymbol{q}_{\text{ext0},\boldsymbol{x}} \tag{C4}$$

and

$$R_{,\lambda} = R_{,\lambda}(\boldsymbol{a}, \boldsymbol{x}) = -\boldsymbol{q}_{\text{ext0}} \tag{C5}$$

Also, $R_{,\boldsymbol{a}}$ is known as the tangential stiffness matrix of the system

$$K_T = K_T(\boldsymbol{a}, \boldsymbol{x}, \lambda) = R_{,\boldsymbol{a}} \tag{C6}$$

which is *nonsymmetric* for a general loading case, e.g., when the pressure load is considered.

Therefore, we can write the *augmented* linearized incremental state equation as

$$R + R_{,\boldsymbol{a}}\Delta\boldsymbol{a} + R_{,\boldsymbol{x}}\Delta\boldsymbol{x} + R_{,\lambda}\Delta\lambda = 0 \tag{C7}$$

The residual vector vanishes at the equilibrium for given load factor λ:

$$R = 0 \tag{C8}$$

Thus, we have the augmented linearized incremental state equation at equilibrium

$$K_T\Delta\boldsymbol{a} + R_{,\boldsymbol{x}}\Delta\boldsymbol{x} = 0 \tag{C9}$$

or

$$K_T\Delta\boldsymbol{a} - \lambda K_T^{-1}\boldsymbol{q}_{\text{ext0},\boldsymbol{x}}\Delta\boldsymbol{x} = 0 \tag{C10}$$

or

$$\boldsymbol{a}_{,\boldsymbol{x}} = \lambda K_T^{-1}\boldsymbol{q}_{\text{ext0},\boldsymbol{x}} \tag{C11}$$

where $\mathbf{a}_{,\mathbf{x}}$ is the sensitivity of displacement vector with respect to the load design vector $\mathbf{x}$ and $\mathbf{q}_{\text{ext0},\mathbf{x}}$ is the global force coefficient matrix, which is obtained by the assembling operation using the relations given in Eqs. (B15–B21).

Appendix D: Derivatives of Strains with Respect to Load (Force) Coefficient Vector

For the translational strain vector in the material form, one has, noticing Sec. III.C of Kapania and Li [43],

$$\begin{aligned}\Delta_x\bar{\boldsymbol{\varepsilon}} = \bar{\boldsymbol{\varepsilon}}_{,x_\alpha}\Delta x_\alpha = \boldsymbol{\Lambda}^t(\Delta_x\boldsymbol{\varphi}_{,\xi_1} + \hat{\boldsymbol{\varphi}}_{,\xi_1}\Delta_x\boldsymbol{w}) = \boldsymbol{\Lambda}^t[(\boldsymbol{\varphi}_{,\xi_1})_{,x_\alpha} \\ + \hat{\boldsymbol{\varphi}}_{,\xi_1}\boldsymbol{w}_{,x_\alpha}]\Delta x_\alpha = (\boldsymbol{e}_j \otimes \boldsymbol{t}_j)[(\boldsymbol{\varphi}_{,\xi_1})_{,x_\alpha} + \hat{\boldsymbol{\varphi}}_{,\xi_1}\boldsymbol{w}_{,x_\alpha}]\Delta x_\alpha = \{\boldsymbol{t}_j \\ \cdot [(\boldsymbol{\varphi}_{,\xi_1})_{,x_\alpha} + \hat{\boldsymbol{\varphi}}_{,\xi_1}\boldsymbol{w}_{,x_\alpha}]\}\boldsymbol{e}_j\Delta x_\alpha\end{aligned} \tag{D1}$$

For the bending strain vector in the material form, one has

$$\begin{aligned}\Delta_x\bar{\boldsymbol{\kappa}} = \bar{\boldsymbol{\kappa}}_{,x_\alpha}\Delta x_\alpha = \boldsymbol{\Lambda}^t\Delta_x\boldsymbol{w}_{,\xi_1} = \boldsymbol{\Lambda}^t(\boldsymbol{w}_{,\xi_1})_{,x_\alpha}\Delta x_\alpha = [\boldsymbol{t}_j \\ \cdot (\boldsymbol{w}_{,\xi_1})_{,x_\alpha}]\boldsymbol{e}_j\Delta x_\alpha\end{aligned} \tag{D2}$$

For the position vector of the midcurve of the deformed beam, one has

$$\Delta_x\boldsymbol{\varphi} = \boldsymbol{\varphi}_{,x_\alpha}\Delta x_\alpha = \Delta_x(\boldsymbol{\varphi}_0 + \boldsymbol{u}) = \Delta_x\boldsymbol{\varphi}_0 + \Delta_x\boldsymbol{u} = \Delta_x\boldsymbol{u} = \boldsymbol{u}_{,x_\alpha}\Delta x_\alpha \tag{D3}$$

$$\Delta_x\boldsymbol{\varphi}_{,\xi_1} = (\boldsymbol{\varphi}_{,\xi_1})_{,x_\alpha}\Delta x_\alpha = (\boldsymbol{\varphi}_{,x_\alpha})_{,\xi_1}\Delta x_\alpha \tag{D4}$$

For the incremental rotation vector, one has

$$\Delta_x\boldsymbol{w} = \boldsymbol{w}_{,x_\alpha}\Delta x_\alpha \tag{D5}$$

and

$$\Delta_x\boldsymbol{w}_{,\xi_1} = (\boldsymbol{w}_{,\xi_1})_{,x_\alpha}\Delta x_\alpha = (\boldsymbol{w}_{,x_\alpha})_{,\xi_1}\Delta x_\alpha \tag{D6}$$

At the element level,

$$(\boldsymbol{\varphi}^e_{,\xi_1})_{,x_\alpha} = N_{I,\xi_1}\boldsymbol{\varphi}^e_{I,x_\alpha} = N_{I,\xi_1}\boldsymbol{u}^e_{I,x_\alpha} \tag{D7}$$

$$\boldsymbol{w}^{\,e}_{,x_\alpha} = N_I\boldsymbol{w}^e_{I,x_\alpha} \tag{D8}$$

$$(\boldsymbol{w}^e_{,\xi_1})_{,x_\alpha} = N_{I,\xi_1}\boldsymbol{w}^e_{I,x_\alpha} \tag{D9}$$

where $N_I = N_I(\xi)$ is the Lagrangian interpolation function of node I.

Acknowledgments

The researchers thank Scott Ragon of Advanced Design and Optimization Technologies, Inc., Jeff Chock of Virginia Polytechnic Institute and State University, Efstratios Nikolaidis of University of Toledo, and Tom Stoumbos of General Dynamics Amphibious Marine Systems for valuable technical discussions.

References

[1] Rattray, R., Burns, D. H., and Salin, E. D., "Peak Fitting and Deconvolution for Determination of the Impulse Response Function of the Sample Introduction System in Flow Injection Inductively Coupled Plasma Spectrometry," *Applied Spectroscopy*, Vol. 53, No. 12, 1999, pp. 1642–1645.

[2] Avitabile, P., "Model-Updating: Endless Possibilities," *Sound and Vibration*, Vol. 34, No. 9, 2000, pp. 20–28.

[3] Chock, J. M. K., and Kapania, R. K., "Load Updating for Finite Element Models," *AIAA Journal*, Vol. 41, No. 9, 2003, pp. 1667–1673.

[4] Engl, H. W., and Kugler, P., "Nonlinear Inverse Problems: Theoretical Aspects and Some Industrial Applications," *Multidisciplinary Methods for Analysis, Optimization and Control of Complex Systems*, Springer–Verlag, New York, 2005, pp. 3–48.

[5] Starkey, J. M., and Merrill, G. L., "Ill-Conditioned Nature of Indirect Force-Measurement Techniques," *Modal Analysis: The International Journal of Analytical and Experimental Modal Analysis*, Vol. 4, No. 3, 1989, pp. 103–108.

[6] Schulze, M., "Parameter Identification for Underdetermined Systems Arising in Option Pricing Models and Neural Networks," Ph.D. Thesis, Mathematik, Universität Trier, 54286 Trier, Germany, Aug. 2002.

[7] Eriksson, J., and Gulliksson, M. E., "Local Results for the Gauss-Newton Method on Constrained Rank-Deficient Nonlinear Least Squares," *Mathematics of Computation*, Vol. 73, No. 248, 2003, pp. 1865–1883.

[8] Snieder, R., "Role of Nonlinearity in Inverse Problems," *Inverse Problems*, Vol. 14, No. 3, 1998, pp. 387–404.

[9] Hansen, P. C., and O'Leary, D. P., "Use of the L-Curve in the Regularization of Discrete Ill-Posed Problems," *SIAM Journal on Scientific Computing*, Vol. 14, No. 6, 1993, pp. 1487–1503.

[10] Elliott, K. B., Juang, J. N., and Robinson, J., "Force Prediction Using Singular Decomposition," *Proceedings of the 6th International Modal Analysis Conference*, Society for Experimental Mechanics, Bethel, CT, 1988, pp. 1582–1588.

[11] Fabunmi, J. A., "Effects of Structural Modes on Vibratory Force Determination by the Pseudoinverse Technique," *AIAA Journal*, Vol. 24, No. 3, 1986, pp. 504–509.

[12] Tikhonov, A. N., and Arsenin, V. Y., *Solutions of Ill-Posed Problems*, Wiley, New York, 1977.

[13] Louis, A. K., "Unified Approach to Regularization Methods for Linear Ill-Posed Problems," *Inverse Problems*, Vol. 15, No. 2, 1999, pp. 489–498.

[14] Andrieuxy, S., and Ben Abda, A., "Identification of Planar Cracks by Complete Overdetermined Data: Inversion Formulae," *Inverse Problems*, Vol. 12, No. 5, 1996, pp. 553–563.

[15] Eller, M., "Identification of Cracks in Three-Dimensional Bodies by Many Boundary Measurements," *Inverse Problems*, Vol. 12, No. 4, 1996, pp. 395–408.

[16] Sabatier, P. C., "Patchwork Approach to Problems with Boundary Measurements," *Inverse Problems*, Vol. 11, No. 6, 1995, pp. 1233–1245.

[17] Kaipio, J. P., Kolehmainen, V., Vauhkonen, M., and Somersalo, E., "Inverse Problems with Structural Prior Information," *Inverse Problems*, Vol. 15, No. 3, 1999, pp. 713–729.

[18] Chen, S. L., and Geradin, M., "Dynamic Force Identification for Beamlike Structures Using an Improved Dynamic Stiffness Method," *SIAM Journal on Computing*, Vol. 3, No. 3, 1996, pp. 183–191.

[19] Ewing, R. E., Lin, T., and Lin, Y., "Mixed Least-Squares Method for an Inverse Problem of a Nonlinear Beam Equation," *Inverse Problems*, Vol. 15, No. 1, 1999, pp. 19–32.

[20] Ring, W., "Identification of the Load of a Partially Breaking Beam from Inclination Measurements," *Inverse Problems*, Vol. 15, No. 4, 1999, pp. 1003–1020.

[21] Dunn, S. A., *Technique for Unique Optimization of Dynamic Finite Element Models*, Academic Press, New York, 1976, p. 426.

[22] Chiroiu, C., Munteanu, L., Chiroiu, V., Delsanto, P. P., and Scalerandi, M., "Genetic Algorithm for Determination of the Elastic Constants of a Monoclinic Crystal," *Inverse Problems*, Vol. 16, No. 1, 2000, pp. 121–132.

[23] Trivailo, P. M., Dulikravich, G. S., Sgarioto, D. E., and Gilbert, T., "Inverse Problem of Aircraft Structural Parameter Estimation: Application of Neural Networks," *Inverse Problems in Science and Engineering*, Vol. 14, No. 4, 2006, pp. 351–363.
[24] Trivailo, P. M., Gilbert, T., Glessich, E., and Sgarioto, D., "Inverse Problem of Aircraft Structural Parameter Identification: Application of Genetic Algorithms Compared with Artificial Neural Networks," *Inverse Problems in Science and Engineering*, Vol. 14, No. 4, 2006, pp. 337–350.
[25] Hanke, M., *Conjugate Gradient Type Methods for Ill-Posed Problems*, Longman Scientific & Technical, Harlow, Essex, England, 1995, Chap. 2.
[26] Rieder, A., "Regularization of Nonlinear Ill-Posed Problems via Inexact Newton Iterations," *Inverse Problems*, Vol. 15, No. 1, 1999, pp. 309–327.
[27] Burger, M., and Muhlhuber, W., "Iterative Regularization of Parameter Identification Problems by Sequential Quadratic Programming Methods," *Inverse Problems*, Vol. 18, No. 4, 2002, pp. 943–969.
[28] Feijoo, G. R., Oberai, A. A., and Pinsky, P. M., "Application of Shape Optimization in the Solution of Inverse Acoustic Scattering Problems," *Inverse Problems*, Vol. 20, No. 1, 2004, pp. 199–228.
[29] Hasanov, A., and Mamedov, A., "Inverse Problem Related to the Determination of Elastoplastic Properties of a Plate," *Inverse Problems*, Vol. 10, No. 3, 1994, pp. 601–615.
[30] Pilkey, W. D., and Kalinowski, J., "Identification of Shock and Vibration Forces," *System Identification of Vibrating Structures and Mathematical Models from Test Data*, American Society of Mechanical Engineers, New York, 1972, pp. 73–86.
[31] Hillary, B., and Ewins, D. J., "Use of Strain Gauges in Force Determination and Frequency Response Function Measurements," *Proceedings of the 2nd Internal Modal Analysis Conference*, Society for Experimental Mechanics, Bethel, CT, 1984, pp. 627–634.
[32] Gregory, D. L., Priddy, T. G., and Smallwood, D. O., "Experimental Determination of the Dynamic Forces Acting on Non-Rigid Bodies," *Aerospace Technology Conference and Expo, Warrendale, PA*, SAE Technical Paper Series, Society of Automotive Engineers Paper 861791, 1986.
[33] Stevens, K. K., "Force Identification Problems: An Overview," *Proceedings of the 1987 Society for Experimental Mechanics Spring Conference on Experimental Mechanics*, Society for Experimental Mechanics, Bethel, CT, 1987, pp. 838–844.
[34] Wang, M. L., Kreitinger, T., and Luo, H. L., "Force Identification from Structural Response," *Proceedings of the 1987 SEM Spring Conference on Experimental Mechanics*, Society for Experimental Mechanics, Bethel, CT, 1987, pp. 851–855.
[35] Park, H., and Park, Y., "Transient Response of an Impacted Beam and Indirect Impact Force Identification Using Strain Measurements," *Shock and Vibration*, Vol. 1, No. 3, 1994, pp. 267–278.
[36] Johnson, C. D., "Necessary and Sufficient Conditions for Unknown Force/Moment Identification," *Southeastern Conference on Theoretical and Applied Mechanics (19th)*, Vol. 19, 1998, pp. 192–203.
[37] Johnson, C. D., "Identification of Unknown, Time-Varying Forces/Moments in Dynamics and Vibration Problems Using a New Approach to Deconvolution," *Shock and Vibration*, Vol. 5, No. 3, 1998, pp. 181–197.
[38] Johnson, C. D., "Identification of Unknown Static Load Distributions on Beams from Measurements," *Southeastern Conference on Theoretical and Applied Mechanics (19th)*, Vol. 19, SECTAM, 1998, pp. 159–171.
[39] Law, S. S., and Fang, Y. L., "Moving Force Identification: Optimal State Estimation Approach," *Journal of Sound and Vibration*, Vol. 239, No. 2, 2001, pp. 233–254.
[40] Chock, J. M. K., and Kapania, R. K., "Finite Element Load Updating for Plates," *45th AIAA/ASME/ASCE/AHS/ASC Structures, Structural Dynamics, and Materials Conference and Exhibit April 19–22, 2004 , Palm Springs, CA*, AIAA Paper 2004-2004, 2004.
[41] Padmanabhan, S., Hubnerand, J. P., Kumar, A. V., and Ifju, P. G., "Load and Boundary Condition Calibration Using Full-field Strain Measurement," *Experimental Mechanics*, Vol. 46, No. 5, 2006, pp. 569–578.
[42] Kapania, R. K., and Li, J., "Geometrically Exact Curved/Twisted Beam Theory under Rigid Cross-Section Assumption," *Computational Mechanics*, Vol. 30, Nos. 5–6, 2003, pp. 428–443.
[43] Kapania, R. K., and Li, J., "Formulation and Implementation of Geometrically Exact Curved Beam Elements Incorporating Finite Strains and Finite Rotations," *Computational Mechanics*, Vol. 30, Nos. 5–6, 2003, pp. 444–459.
[44] Byrd, R. H., Lu, P., Nocedal, J., and Zhu, C., "Limited Memory Algorithm for Bound Constrained Optimization," *SIAM Journal on Computing*, Vol. 16, No. 5, 1995, pp. 1190–1208.
[45] Zhu, C., Byrd, R., Lu, P., and Nocedal, J., "L-BFGS-B: FORTRAN Subroutines for Large Scale Bound Constrained Optimization," Northwestern Univ., Tech. Rept. NAM-11, Electrical Engineering and Computer Sciences Dept., Feb. 1994.
[46] Solin, P., *Partial Differential Equations and the Finite Element Method*, Wiley, New York, 2005, Chap. 2.
[47] Szabo, B., and Babuska, I., *Finite Element Analysis*, Wiley, New York, 1991, Chap. 4.
[48] Banks, H. T., "Tutorial on Differential Equation Modeling and Inverse Problems," *Inverse Problem Methodology in Complex Stochastic Models Sept. 2002–Jan. 2003*, Statistical and Applied Mathematical Sciences Inst., http: //www.samsi.info/talks/inverse/Inverse-Banks.pdf, [Retrieved 2004].
[49] Miller, R. G., *Beyond ANOVA: Basics of Applied Statistics*, Chapman & Hall, Boca Raton, FL, 1997, Chap. 1.
[50] Bates, D. M., and Watts, D. G., *Nonlinear Regression and Its Applications*, Wiley, New York, 1988, Chap. 1.

A. Palazotto
Associate Editor